University Turbine Systems Research (UTSR)
Industrial Fellowship Program
2013

Final Report

Phantom Cooling Studies in a Gas Turbine Engine

Prepared For:

Solar Turbines, Inc.
Mentor: Dr. Luzeng Zhang
2200 Pacific Highway
San Diego, CA 92186

&

Southwest Research Institute (SWRI)
Mechanical Engineering Division
6220 Culebra Road
San Antonio, TX 78238

Prepared By:

Matthew E. Stinson
Graduate Research Assistant
University of Minnesota
Minneapolis, MN 55455

1 Introduction

In modern gas turbine engines, high combustor exit temperatures are used to increase engine power output and engine thermal efficiency. However, at these higher temperatures, turbine blades and vanes are more prone to failure. Film-cooling is used to protect the turbine surfaces and prevent failure due to the extreme thermal conditions. In film-cooling, cool air is bled from the compressor stage and is discharged through the turbine walls that are to be cooled. This air forms an insulating layer along the turbine walls that protects against the hot mainstream fluid. In general, the cool air is discharged at or directly upstream of the surfaces that are to be cooled. However, this coolant has the potential to cool secondary, potentially unintended, surfaces. This cooling effect is referred to as phantom cooling, in which film coolant cools secondary surfaces. Some examples of phantom cooling are as follows: (1) First stage vane coolant cooling the downstream first stage blade surfaces, (2) First stage blade coolant cooling the downstream second stage vane surfaces, (3) Vane or blade surface coolant cooling the adjacent endwall surface, and (4) Endwall surface coolant cooling the adjacent vane or blade surfaces.

In the film-cooling literature, there are few studies on phantom cooling. It is usually assumed to be an insignificant effect, so it is usually ignored in the design of a turbine cooling scheme. However, with continual advances and optimizations in turbine cooling, previously less important considerations are becoming more important to fully optimize turbine cooling. Therefore, more attention is being paid towards previously ignored or neglected cooling considerations such as phantom cooling.

In this report, two phantom cooling studies are discussed. The first study is on cooling air discharged from the vane surface which cools the adjacent endwall surface. This study is experimental and uses the pressure sensitive paint (PSP) technique to analyze the phantom cooling effect. Additionally, due to PSP measurement challenges at high mainflow temperatures, an overhaul of the wind tunnel facility is planned in order to cool the mainflow air. The second study is on cooling air discharged from a first stage vane surface which cools the downstream surface of a first stage blade. This study uses computational fluid dynamics (CFD) to predict the phantom cooling effect.

2 PSP Study

The pressure sensitive paint (PSP) technique is used to study the phantom cooling effect on the endwall surface with coolant discharged from the adjacent vane surfaces.

The airfoil shape used in this study is representative of a typical, high-performance, modern first stage vane design. The scaled cascade facility at Solar Turbine Incorporated will be used for this study. In the tunnel, a single passage on the cascade is painted with pressure sensitive paint, which is where the adiabatic wall effectiveness for the phantom cooling will be determined. A parametric study was performed with the following parameters as variables: (1) the mass flow ratio (MFR), (2) the distance between the endwall and the first hole on the vane surface (the first pitch), (3) the injection angles on the vanes, and (4) the vane injection locations (pressure side, suction side, or both sides).

2.1 Theory

Pressure sensitive paint is comprised of an oxygen permeable binder that contains fluorescent molecules. When incident light at a specific wavelength is directed to the pressure sensitive paint, the luminescent molecule fluoresces. The intensity of

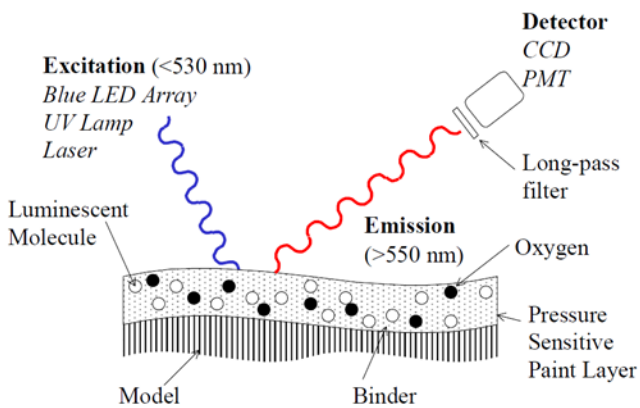

Figure 2.1: A pressure sensitive paint detection system.

the fluorescence varies with the partial pressure and temperature of local oxygen molecules. In practice, the light intensity is calibrated against both temperature and pressure in a form such as in equation (2.1).

$$\frac{I_{ref}}{I} = A(T) + B(T)(\frac{P}{P_{ref}}) + C(T)(\frac{P}{P_{ref}})^2 + ... \tag{2.1}$$

Finally, during the actual experiment, the camera will return the luminescent intensity values locally as a function of position. These light intensity values can be related to the local partial pressure of oxygen by the calibration.

To determine the adiabatic wall effectiveness from local partial pressure values of oxygen, the heat-mass transfer analogy is utilized. Two experiments are performed: one with air as the "coolant," and the other with nitrogen as the "coolant." The significance of the nitrogen case is that the concentration of oxygen is zero, so the adiabatic wall effectiveness simplifies to equation (2.2).

$$\eta = 1 - \frac{(P_{O_2})_{N_2\ injection}}{(P_{O_2})_{air\ injection}} \tag{2.2}$$

2.2 Test Facility

The experiments are performed in a high-performance compressible flow wind tunnel detailed in figure 2.2. Outdoor air is drawn in through a inlet filter and then compressed adiabatically by way of a four-stage centrifugal compressor. The compressed

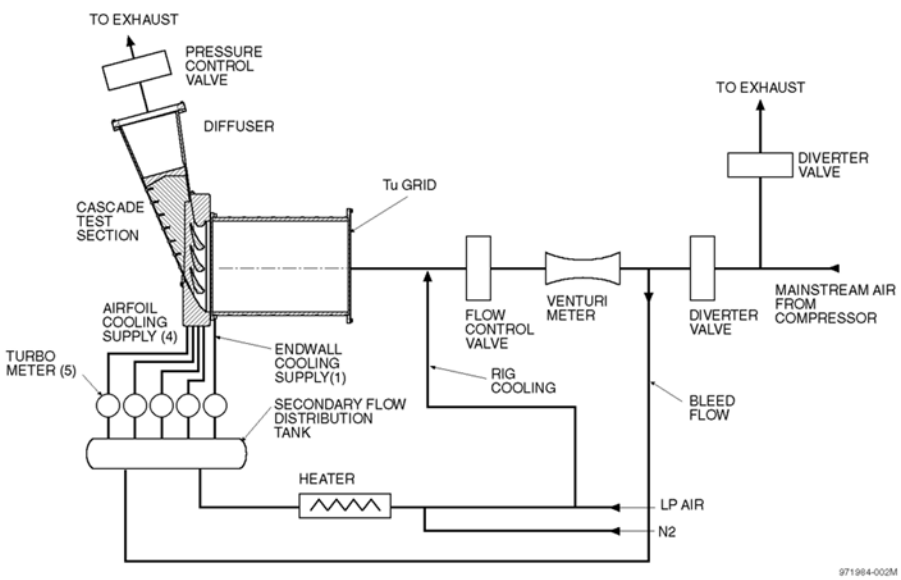

Figure 2.2: Schematic of scaled cascade rig.

air then enters into the facility. By controlling three diverter valves, three objectives can be accomplished: (1) the compressor can be kept near the maximum efficiency operating point, well away from surge and choked flow, (2) the Reynolds number can be specified, and (3) the Mach number can be specified.

2.3 Experimental Results

A subset of the experimental results are presented in figure 2.3. The results show the trend of phantom cooling on the endwall surface as the mass flow ratio (MFR) is increased. In this set of runs, vane I showerhead and suction side injection, and vane II showerhead and pressure side injection are all present. The active endwall region is clearly indicated between the two vanes and is bordered by the thick black lines.

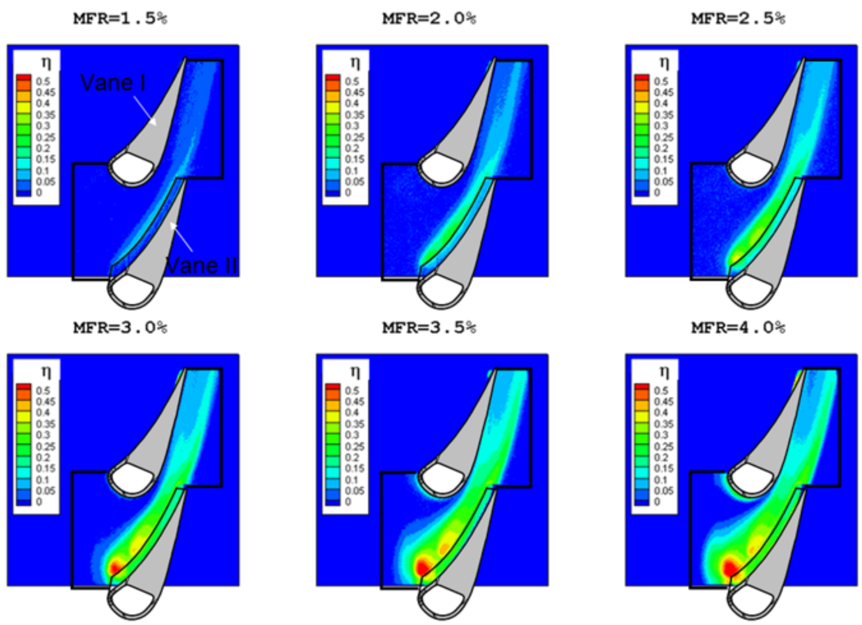

Figure 2.3: Endwall adiabatic wall effectiveness for vane I showerhead and suction side injection, and vane II showerhead and pressure side injection.

While this is only a small subset of the complete set of results in this study, it shows the most important trends and findings. First, it was found that the pressure side injection had a much greater phantom cooling effect than the suction side injection. This is expected due to the endwall crossflow present which sweeps flow from pressure to suction side. Only in the very high MFR cases was the suction side injection over to overcome the crossflow. The second major finding is that the MFR is the most important parameter which determines the significance of the phantom cooling effect on the adjacent endwall. For typical values found in an engine closer to 2 %, a moderately sized area of the endwall surface is significantly cooled, whereas around 4 %, the vast majority of the endwall surface is significantly cooled. The third major finding is that, generally speaking, the phantom cooling effect from pressure side coolant injection on the adjacent endwall surface is a non-negligible effect. This means that if these results are utilized properly, the turbine cooling scheme could be further optimized by a significant margin in these regions.

2.4 Scaled Cascade Heat Exchanger Addition

In the past 18 months, the compressor for the scaled cascade facility was upgraded. This was beneficial for the project in that it brought the Reynolds number and Mach number closer to real engine conditions. However, the upgraded compressor undergoes a more significant pressure rise, which gives rise to larger mainflow temperatures in the tunnel due to the increased heat of compression. This poses a problem for the pressure sensitive paint technique. At greater temperatures, less light intensity is observed and the resulting images are relatively noisier. This issue is amplified in the summer when the compressor inlet temperatures are increased. Since the compressor upgrade was been completed, quality pressure sensitive paint results have only been achievable in the winter time. Therefore, it was decided to add a system to cool the air temperature in the tunnel, such as a heat exchanger.

2.4.1 Heat Exchanger Requirements

In order to design and select a heat exchanger, specific requirements were required. The following represent the primary requirements for the heat exchanger: (1) handle up to 7000 SCFM of air, (2) cool air by at least 30 °F or below 170 °F, and (3) limit the air side pressure drop to 0.5 psi.

2.4.2 Heat Exchanger Design

There were two key decisions involved in designing the heat exchanger to cool the airflow in the scaled cascade rig: the type of heat exchanger and the type and source for the coolant. Since these decisions cannot be made independently, the decision making process was iterative.

Selected Heat Exchanger

An air-to-water finned-tube heat exchanger was selected as deoicted in figure 2.4. A finned tube design is a typical, economical design for cooling air. The primary alternatives were shell-and-tube (not as economic) designs or air-to-air (not as space efficient) cooling designs.

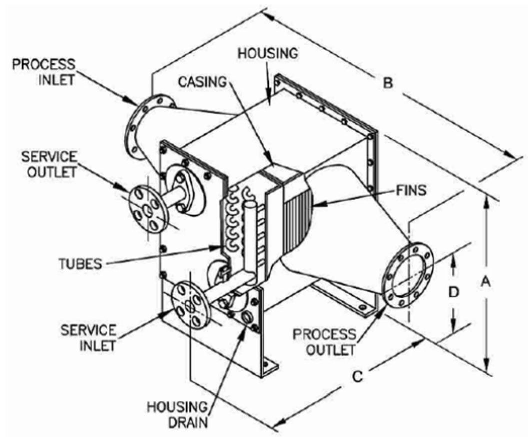

Figure 2.4: Xchanger Inc., C-275 Fin-Tube Core Heat Exchanger.

Coolant Source Selection

It was decided to use a cooling tower water source that is currently in service at Solar Turbines as depicted in figure 2.5. The primary alternative would have been a closed

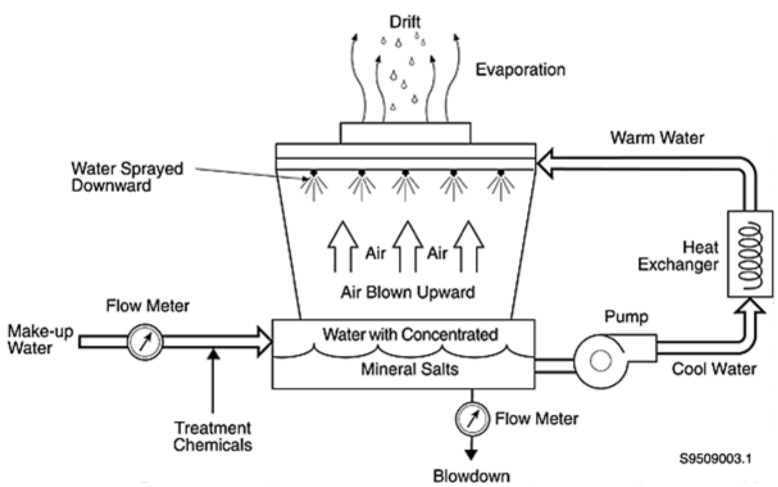

Figure 2.5: Schematic of the cooling tower water loop and operation.

loop chiller unit. Since the temperature drop requirement was not significant, there is little thermal advantage to using the chiller unit. The primary advantage in the chiller unit is decreased fouling in the closed water loop. The primary disadvantage is greatly increased costs, both upfront and ongoing. Considering the pros and cons, it was determined that the cooling tower made the most sense.

2.4.3 Heat Exchanger Performance

The heat exchanger's thermal performance is predicted for various levels of fouling in figure 2.6. For all reasonable fouling levels, the required performance specifica-

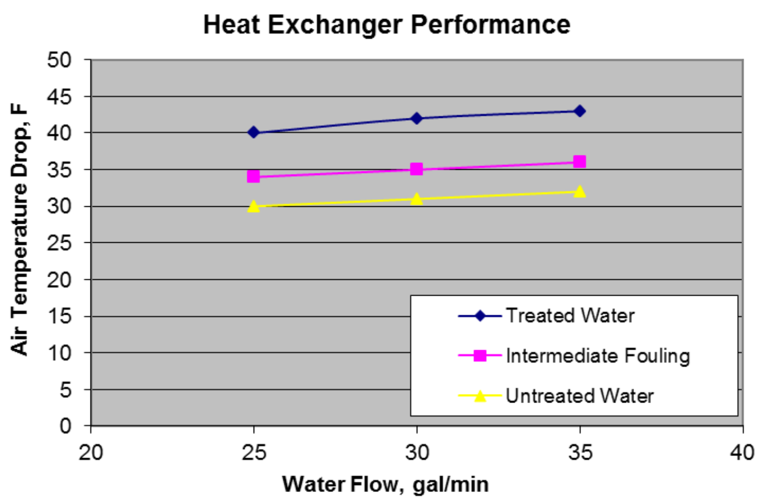

Figure 2.6: Heat exchanger temperature drop for various water flow rates and fouling factors.

tions are met. If the cooling tower unit is maintained properly, the heat exchanger performance should follow close to the "Treated Water" curve, however, it is noted that due to high dissolved salt concentrations in the cooling tower loop, scaling is a concern and the performance may likely be closer to the "Intermediate Fouling" case. At 8000 SCFM, the pressure drop through the heat exchanger is only 0.07 psi, which is more than adequate and won't significantly affect the performance in scaled cascade rig.

3 CFD Study

The computational fluid dynamics software ANSYS CFX is used to study the phantom cooling effect on the blade surface cooled by spent cooling from an upstream vane. The airfoil shape used in this study is representative of a typical, high-performance, modern first stage blade design. The only parameter that is varied is the coolant injection velocity ratio from the upstream vane, which also changes to relative coolant approach angle. Note that while the velocity ratio is changed, the coolant mass flow is fixed. A subset of the flow domain is shown in figure 3.1. Note

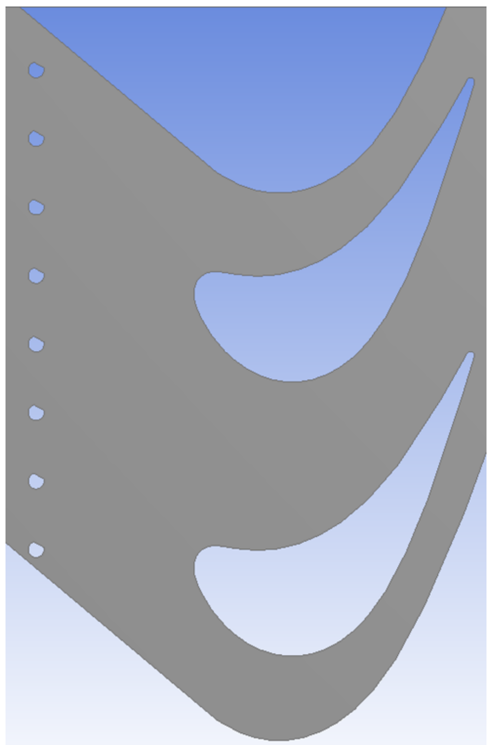

Figure 3.1: CFD model volume.

that the eight upstream holes represent the coolant injection locations for this study. A static mesh is used to simulate the actual rotating engine, and only one hole is activated at once, so there are eight cases per each upstream coolant injection velocity ratio. The results from these eight cases are averaged to determine the approximate performance for the rotating rig.

3.1 Results

The results for the case when hole 3 is activated is shown in figure 3.2. In this case, it

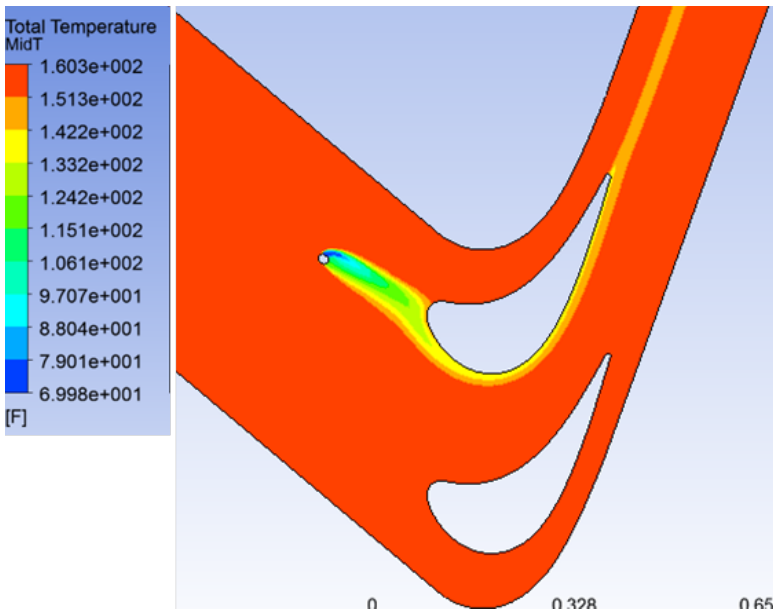

Figure 3.2: Temperature contour at blade mid-span for cooling hole three activated.

can be seen that the upstream coolant has a significant cooling effect on the suction side of the top blade. Note that this is an atypical case, and that on average the upstream coolant does not cool the blade wall to this extent. The adiabatic wall effectiveness is calculated using the proper compressible definition shown in equation (3.1).

$$\eta = \frac{T_{aw} - T_{\infty r}}{T_{c0} - T_{\infty r}} \tag{3.1}$$

The final results are shown in figure 3.3. It was found that the lowest upstream velocity ratio case, $VR = 0.4$, leads to the greatest film cooling effect. This may be surprising at first glance, as, typically, greater velocity ratios, and thus momentum ratios, lead to improved film-cooling. The explanation is that the lower velocity ratio case actually corresponds to the greater *relative* velocity ratio, which is more physically significant than the velocity ratio defined from two different reference frames. Generally, the coolant did a very poor job at cooling the pressure side of the downstream blade surfaces, with the adiabatic wall effectiveness values falling roughly below 1 % for all three cases. The coolant did a better job at cooling the

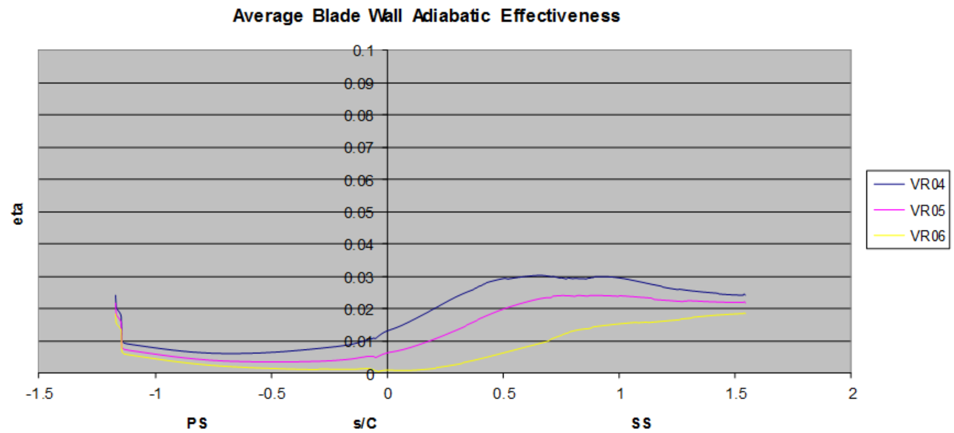

Figure 3.3: Adiabatic wall effectiveness for three velocity injection ratios.

suction side surfaces with adiabatic wall effectiveness values approaching 3 % for the lowest velocity ratio. However, overall, it was found that the phantom cooling of a downstream blade from the upstream spent coolant on a vane is a very weak effect and is likely not significant enough to consider in designing a turbine cooling scheme.

4 Conclusions

With the push to continually optimize and approach the limits on cooling schemes in gas turbine engines, less significant cooling phenomena, such as phantom cooling, are beginning to receive attention in recent literature. The hypothesis going into these phantom cooling studies "Treated Water"was that phantom cooling was an insignificant effect and was not worth accounting for. For phantom cooling on a downstream blade from spent upstream coolant, it is indeed arguable that the cooling effect is too weak to be worth considering. However, for the phantom cooling effect in which vane wall coolant cools the adjacent endwall, the effect is significant and worth accounting for in designing an endwall cooling scheme. In general, a more optimized cooling scheme leads to a more reliable gas turbine and/or greater turbine efficiencies and power output, so these small incremental potential improvements to a gas turbine cooling scheme are always worth considering and studying.

5 Acknowledgments

The author would like to thank the Southwest Research Institute (SWRI) and the University Turbine Systems Research (UTSR) program for making this fellowship opportunity possible. The fellowship was an invaluable opportunity for the author and provided a complimentary experience to the academic gas turbine research he is currently involved in.

The author would also like to thank various individuals at Solar Turbines Incorporated: John Mason and Dr. Hee-Koo Moon for their support and help while part of the Aero/Thermal & Performance group at Solar Turbines Incorporated. The author would especially like to thank his mentor, Dr. Luzeng Zhang, and Gail Doore for their significant help, guidance, and instruction during the course of the fellowship.